Modeling of Degradation Mechanism at the Oil-Pressboard Interface due to Surface Discharge

H. Zainuddin[*1] and P. L. Lewin[2]

[1]Research Laboratory of High Voltage Engineering, Faculty of Electrical Engineering, Universiti Teknikal Malaysia Melaka, Hang Tuah Jaya, 76100 Durian Tunggal, Melaka, Malaysia
[2]The Tony Davies High Voltage Laboratory, University of Southampton, Southampton SO17 3AS, United Kingdom
*Corresponding author: hidayat@utem.edu.my

Abstract: Surface discharge at the oil-pressboard interface results in creeping path (tracking) in the form of white marks and carbonisation of the oil and cellulose from the discharge source towards the earth electrode. In order to understand these degradation marks, a finite element model is developed by using COMSOL Multiphysics. The charge transport equations are coupled with the Poisson's and heat transfer equations to simulate the electric field distribution during the streamer propagation and to investigate the drying mechanism at the oil-pressboard interface. The simulation results provide a reasonable argument behind the formation of white and carbonised marks during the surface discharge experiment as a result of drying out process. The results have associated both degradation marks on pressboard surface with high energy of long periods of partial discharge event that leads to thermal degradation at the oil-pressboard interface.

Keywords: surface discharge, partial discharge, oil-pressboard interface, degradation, tracking.

1. Introduction

Surface discharge is a type of partial discharge at the interface of oil-impregnated cellulose-based pressboard within power transformer. It is classified as a serious fault condition as it can occur under normal operating conditions [1]. It can continue from minutes to months or even years, until the creeping conductive path or also known as tracking becomes an essential part of a powerful arc [2]. The tracking appears in the form of white and carbonised marks on the pressboard surface from the discharge source towards the earth electrode [3], [4]. Generally, the formation of these degradation marks is believed due to drying out and carbonisation processes during surface discharges at the oil-pressboard interface [5], [6].

This paper presents a finite element model of surface discharge at the oil-pressboard interface that is developed using COMSOL Multiphysics. The model geometry has three media, i.e. the bulk oil region, transition region and bulk oil/pressboard region. In this work, three charge carriers, i.e. positive and negative ions and electrons are considered using charge transport equations to model the discharge streamer. These equations are coupled with the Poisson's and heat transfer equations to simulate the electric field distribution during the streamer propagation and to investigate the drying mechanism at the oil-pressboard interface respectively.

2. Model Representation

This section describes the surface discharge model in terms of the geometry and governing equations.

2.1 Simulation Model Geometry

The surface discharge at the oil-pressboard interface is modelled using a 2-D axial symmetry plane as shown in Figure 1. The oil-pressboard interface considers the physical model illustrated in Figure 2 proposed in [7]. However, the no-slip region which is also called the compact layer in the oil region that is very close to the pressboard surface is neglected in the simulation model. This is because this layer is too small which is characterised by a thickness of a few ions [8], i.e. in the order of 1×10^{-10} m.

The needle tip is drawn with a radius of 70 μm; based on the effective needle tip after 2 to 4 hours of high voltage application during the surface discharge experiment that had a needle radius of approximately 1-3 μm prior to voltage application [9]. The proposed model geometry has three media, i.e. the bulk oil region, a transition region and the bulk oil/pressboard region, whereby the transition region is treated as

the porous part of the pressboard so that the streamer can be modelled to propagate through it. On the other hand, the bulk oil/pressboard region is assumed as a perfect insulator, i.e. this region is assigned zero conductivity ($\sigma = 0$).
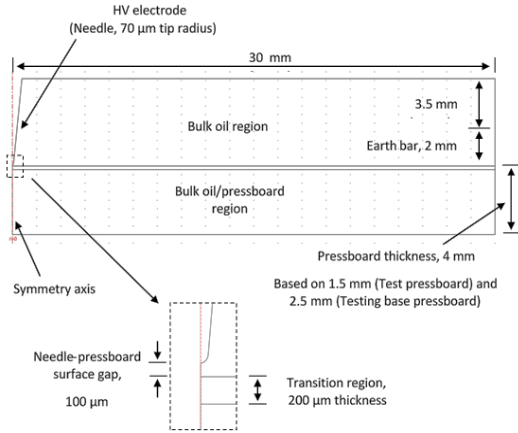
Figure 1. Model geometry for surface discharge simulation using the 2-D axial symmetry plane.
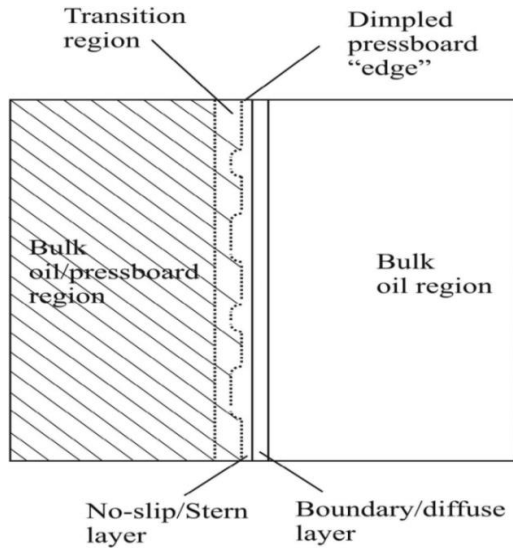
Figure 2. Physical model of the oil-pressboard interface [7].

2.2 Governing Equations in Bulk Oil and Transition Regions

In order to model the surface discharge at the oil-pressboard interface which involves streamer propagation in the oil and transition regions, the governing equations for both regions are based on the charge transport continuity equations:

$$\frac{\partial N_i}{\partial t} + \nabla \cdot \vec{F}_i = G_i - R_i \tag{1}$$

where N_i is the density of each charge carrier (mol·m^{-3}), i.e. positive ion, N_p or negative ion, N_n or electron, N_e and $\vec{F}_i$ is the total flux density vector (mol·m^{-2}·s^{-1}) due to the movement of each charge carrier. The right hand side of the charge continuity equation depicted in Equation (1) is the source term (mol·m^{-3}·s^{-1}) which depends on the generation rate, G_i and recombination rate, R_i of the ionic species.

The surface discharge streamer is assumed to be dominated by conduction currents. Thus, in the model, the total flux only considers the electro-migration of each charge carrier due to the influence of the electric field and neglects any charge carrier movements due to diffusion process and fluid convection. Hence, the total flux density vector for each charge carrier can be expressed as:

$$\vec{F}_i = \pm N_i \mu_i \vec{E} \tag{2}$$

where $\vec{E}$ is the electric field vector (V·m^{-1}) and μ_i is the mobility (m^2·s^{-1}·V^{-1}) for each charge carrier. The '$\pm$' sign accounts for the direction of charge migration, whereby, the '+' sign is used for positive ion and the '$-$' sign is used for negative polarity charge carriers (negative ion and electron).

In an earlier work, Devins et al [10] have successfully applied the Zener model [11] to qualitatively explain the propagation of positive streamer in dielectric liquid from their experimental results. Validation works using the COMSOL Multiphysics Simulation package [12], [13] have shown that field dependent molecular ionisation plays a dominant role in pre-breakdown streamer development in transformer oil. The Zener model can be expressed as:

$$G_i(|\vec{E}|) = \frac{q N_0 a |\vec{E}|}{h} exp\left(-\frac{\pi^2 m^* a \Delta^2}{q h^2 |\vec{E}|}\right) \tag{3}$$

where $G_i(|\vec{E}|)$ is the charge generation rate (mol·m^{-3}·s^{-1}) for positive ion and electron, q is the elementary charge (1.6022×10^{-19} C), N_0 is the density of the ionisable species (mol·m^{-3}), a is the molecular separation distance (m), h is the Planck's constant (6.626×10^{-34} J·s), m^* is the effective electron mass (kg) and Δ is the molecular ionisation energy (J).

Based on the mechanism of field dependent molecular ionisation, it is assumed that a free electron and a positive ion are extracted from a neutral molecule as a result of a sufficiently high electric field. Hence, the charge generation follows this relationship:

$$G_i(|\vec{E}|) = G_p(|\vec{E}|) = G_e(|\vec{E}|) \qquad (4)$$

where $G_p(|\vec{E}|)$ and $G_e(|\vec{E}|)$ are the generation rates (mol·m^{-3}·s^{-1}) for positive ions and electrons correspondingly.

In addition to the generation mechanism, the generated charge carriers are also subject to recombination processes. The possible recombination processes that may occur include recombination between positive and negative ions, R_{pn}, recombination between positive ions and electrons, R_{pe} and electron attachment with neutral molecules, EA to form negative ions and reduce the number of electrons. Each recombination rate can be expressed as:

$$R_{pn} = N_p N_n K_{rpn} \qquad (5)$$

$$R_{pe} = N_p N_e K_{rpe} \qquad (6)$$

$$EA = \frac{N_e}{\tau_a} \qquad (7)$$

where τ_a is the time constant (s) for the electron attachment and K_{rpn} and K_{rpe} are the recombination coefficients (m^3·s^{-1}·mol^{-1}) between positive and negative ions and between positive ions and electrons respectively determined using Langevin's equation [14]:

$$K_{rpn} = \frac{q}{\varepsilon_0 \varepsilon_r}(\mu_p + \mu_n)N_A \qquad (8)$$

where μ_p and μ_n are the mobility (m^2·s^{-1}·V^{-1}) for positive and negative ions respectively.

In order to determine the electric field distribution, the charge transport equations for each charge carrier are coupled with Poisson's equation:

$$\nabla \cdot (-\varepsilon_0 \varepsilon_r \vec{E}) = (N_p - N_n - N_e)q N_A \qquad (9)$$

where ε_0 and ε_r are the permittivity of free space (8.854×10^{-12} F·m^{-1}) and relative permittivity of the material respectively, N_p, N_n and N_e are the density of positive ions, negative ions and electrons (mol·m^{-3}) respectively and N_A is the Avogadro's number (6.023×10^{23} mol^{-1}).

In order to study the degradation behaviour due to drying process as a result of electrical discharge, the heat transfer equation is:

$$\frac{\partial T}{\partial t} = \frac{1}{\rho C_P}\left(k_T \nabla^2 T + \vec{E} \cdot \left(\sum |\vec{F_l}|\right) q N_A\right) \qquad (10)$$

where ρ is the mass density (kg·m^{-3}), C_P is the specific heat capacity (J·kg^{-1}·K^{-1}), k_T is the thermal conductivity (W·m^{-1}·K^{-1}) of the material and T is the temperature (K). The first term on the right hand side of Equation (10) equates to the heat conduction as a result of thermal diffusivity. The second term on the right hand side of the equation represents the heat source from the electrical power dissipation as a result of conduction current heating from the movement of charge carriers during the partial discharge under the influence of local electric field.

2.3 Governing Equations in Bulk Oil/Pressboard Region

With the assumption that the bulk oil/pressboard region is a perfect insulator, the charge transport equations are not applicable in the modelling of this region. Hence, the current through the bulk oil/pressboard region is only a displacement current, i.e. conduction current in this particular region is equal to zero. The governing equations for this region are:

$$\nabla \cdot (-\varepsilon_0 \varepsilon_r \vec{E}) = 0 \qquad (11)$$

$$\frac{\partial T}{\partial t} = \frac{1}{\rho C_P}(k_T \nabla^2 T) \qquad (12)$$

2.4 Boundary Conditions

The boundary conditions imposed for each governing equation are based on the boundaries labelled in Figure 3. Table 1 summarises the boundary conditions for each governing equation. Based on Figure 3, boundary 6 is the boundary between the transition region and bulk oil/pressboard region. With an assumption that the free charge carriers will across this boundary, the continuity equation for the surface charge density N_s (mol·m^{-2}) can be determined from the difference in normal total flux density between both regions. Since the bulk oil/pressboard region is modelled as a perfect insulator, the flux density in the bulk oil/pressboard region is omitted. Thus, the continuity equation can be expressed as:

$$\frac{\partial N_s}{\partial t} = \hat{n} \cdot \left(\sum \left| \overrightarrow{F_{i\_trans}} \right| \right) \qquad (13)$$

where $\frac{\partial N_s}{\partial t}$ is the time derivative of the surface charge density (mol·m^{-2}·s^{-1}), $\overrightarrow{F_{i\_trans}}$ is the total flux density vectors (mol·m^{-2}·s^{-1}) in the transition region. Modelling surface charge is done by integrating Equation (13) over time using the "Weak Form Boundary" application mode in the COMSOL Multiphysics.

For the charge transport equation, conditional boundary conditions [15] have been set at boundary 6. The normal component of the total positive ion flux density vector is:

$$\hat{n} \cdot \overrightarrow{F_p} = \begin{cases} 0 & if \quad \hat{n} \cdot \vec{E} < 0 \\ \hat{n} \cdot \left| \overrightarrow{F_p} \right| & if \quad \hat{n} \cdot \vec{E} \geq 0 \end{cases} \qquad (14)$$

The normal component of the total negative ion flux density vector is:

$$\hat{n} \cdot \overrightarrow{F_n} = \begin{cases} \hat{n} \cdot \left| \overrightarrow{F_n} \right| & if \quad \hat{n} \cdot \vec{E} \leq 0 \\ 0 & if \quad \hat{n} \cdot \vec{E} > 0 \end{cases} \qquad (15)$$

The normal component of the total electron flux density vector is:

$$\hat{n} \cdot \overrightarrow{F_e} = \begin{cases} \hat{n} \cdot \left| \overrightarrow{F_e} \right| & if \quad \hat{n} \cdot \vec{E} \leq 0 \\ 0 & if \quad \hat{n} \cdot \vec{E} > 0 \end{cases} \qquad (16)$$
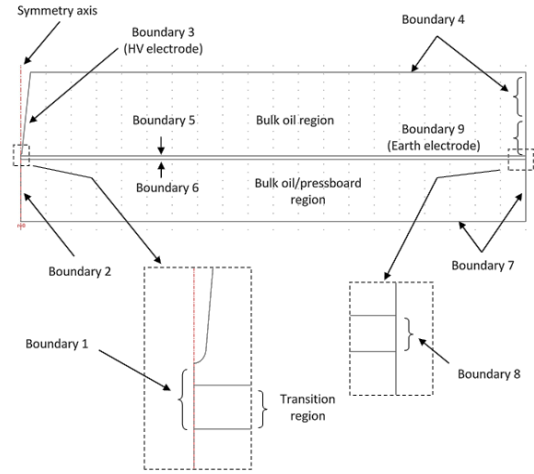

Figure 3. Boundary numbers for the model geometry

Table 1: Boundary conditions for the model

Governing Equation	Charge Transport	Poisson's	Heat Conduction
Boundary 1	Axial symmetry $r = 0$	Axial symmetry $r = 0$	Axial symmetry $r = 0$
Boundary 2	NA		
Boundary 3	$\hat{n} \cdot (-D_i \nabla N_i) = 0$	$V = V_{app}$	
Boundary 4	$\hat{n} \cdot \overrightarrow{F_t} = 0$	$\hat{n} \cdot \vec{D} = 0$ Where, $\vec{D} = \varepsilon_0 \varepsilon_r \vec{E}$	$-\hat{n} \cdot (-k_T \nabla T) = 0$
Boundary 5	$\hat{n} \cdot (\overrightarrow{F_1} - \overrightarrow{F_2}) = 0$	$\hat{n} \cdot (\overrightarrow{D_1} - \overrightarrow{D_2}) = 0$	$\hat{n} \cdot (\overrightarrow{Q_1} - \overrightarrow{Q_2}) = 0$ Where, $\vec{Q} = -k_T \nabla T$
Boundary 6	$\hat{n} \cdot \overrightarrow{F_t} = F_0$ Refer Equation (14)-(16) for details.	$\hat{n} \cdot (\overrightarrow{D_1} - \overrightarrow{D_2}) = N_s q N_A$ Refer Equation (13) for details.	$\hat{n} \cdot (\overrightarrow{Q_1} - \overrightarrow{Q_2}) = Q_s$ Refer Equation (17) for details.
Boundary 7	NA	$\hat{n} \cdot \vec{D} = 0$	$-\hat{n} \cdot (-k_T \nabla T) = 0$
Boundary 8	$\hat{n} \cdot \overrightarrow{F_t} = 0$		
Boundary 9	$\hat{n} \cdot (-D_i \nabla N_i) = 0$	$V = 0$	

If the surface charge, N_s as a result of positive and negative ions and electrons attached to boundary 6 is assumed to have only one value of mobility, the electrical power dissipation on the surface, Q_s (W·m^{-2}) caused by the conduction of surface charges at the boundary can be expressed as:

$$Q_s = \vec{E} \cdot \left(N_s \mu_s \vec{E}\right) q N_A \qquad (17)$$

where μ_s is the surface charge mobility (m^2·s^{-1}·V^{-1}).

3. Results and Analysis

The surface discharge behaviour at the oil-pressboard interface is studied by validating the simulation result with the experimental data by means of surface discharge current pulse. The surface discharge model was solved over a time range of 3 μs. Based on the short period of current pulse, any AC voltage variation is neglected. Thus, a positive DC voltage V_{app} of 30√2, representing the positive peak of AC voltage was applied in the model. Figure 4 shows the comparison between the experimental data and the simulated current pulse. The model appears to have a good agreement with the experimental pulse in terms of the rising front. However, the simulated current decays at a faster rate compared to the decaying tail of the experimental current pulse.
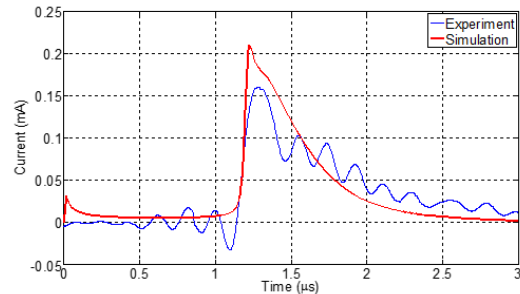
Figure 5 shows the simulation results of temperature distribution along the pressboard surface. Based on the figure, the hottest spot at a particular time appears at the tip of streamer along the pressboard surface, and it is about 12.3 μm apart from the needle tip. The results indicate that streamer branch on the pressboard surface causes significant temperature increase at a spot that is vicinity of needle tip.

Figure 6 shows the variation of temperature at the hottest spot on the pressboard surface. The figure shows that the temperature increases significantly up to about 650 K within 0.2 μs. Then, it increases gradually to approximately 697 K before it decreases gradually to about 650 K. These values are beyond the temperature level that may cause carbonisation of cellulose through dehydration and pyrolysis processes, i.e. less than 500 K [16]. Therefore, the simulated temperatures of the hottest spot on pressboard

surface provide a reasonable argument behind the formation white and black marks during the surface discharge experiment as a result of drying out and ionisation processes. The results suggest that concentration of high temperature over a long period of surface discharges would enhance the carbonisation of cellulose pressboard particularly at the vicinity of needle tip as observed in the surface discharge experiment [3], [4].

In order to aid further understanding on the temperature variation at the hottest spot with respect to time, it is necessary to correlate the temperature variation with the dissipated energy from the generated space charges. The temperature variations are solved using Equation (10) whereby, the electrical power dissipation term is proportional with the rate of temperature variation. By neglecting the thermal conduction term to simplify the solution and performing time integration, the cumulative energy density as a result of electrical power dissipation from the generated charges is determined and shown in Figure 7. Correlation between Figures 6 and 7 suggests that the significant growth of energy dissipation causes the temperature to increase substantially to a certain magnitude. The moment when the energy increases steadily, the temperature starts to decrease gradually. This gradual decrease is caused by the thermal dispersion in the system which is governed by the thermal conductive term in Equation (10).

It is worthwhile noting that the hottest spot on the pressboard surface occupies a very small volume of the transition region. For instance, the hottest spot with the temperature value of 697 K (at the time of 1.7 μs) occupies approximately 3.77×10^{-22} m^3 of the transition region.
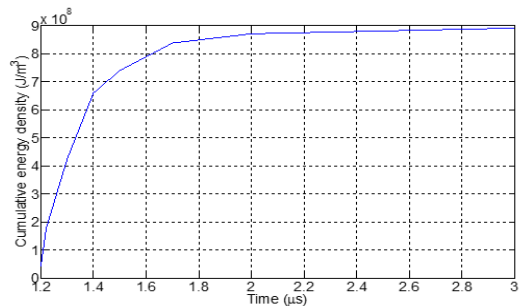

Figure 4. Comparison between experimental and simulation results of surface discharge
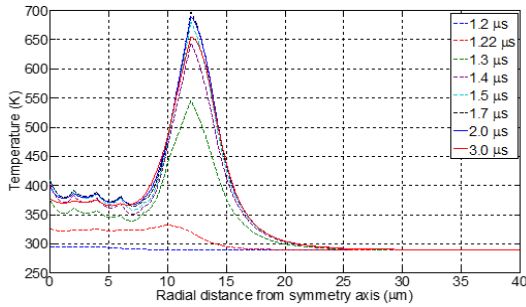
Figure 5. Temperature distribution along boundary 5
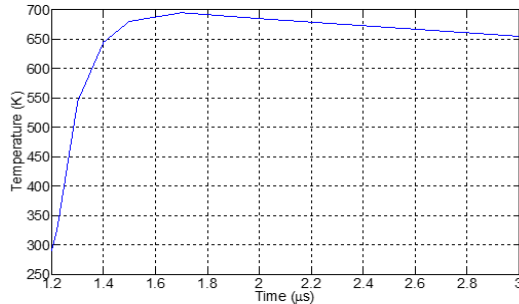
Figure 6. Variation of temperature at the hottest spot with respect to Figure 5

Figure 7. Cumulative energy density calculated from the electrical power dissipation term in Equation (10)

4. Conclusions

A model has been developed using COMSOL Multiphysics to study the degradation behaviour of surface discharge at the oil-pressboard interface at the positive half cycle of AC voltage. The surface discharge behaviour was investigated by validating the simulation results against experimental data of surface discharge current pulse. The results support the hypotheses about the localised nature observed in the experiment of surface discharge at the oil-pressboard interface. These include the development of white marks on the pressboard surface and the formation of carbonised marks that predominantly appear on the pressboard surface at the vicinity of needle tip. The simulation results have associated both degradation marks on pressboard surface with high energy of long periods of partial discharge event that leads to thermal degradation at the oil-pressboard interface.

5. References

1. V. Sokolov, Z. Berler, and V. Rashkes, "Effective methods of assessment of insulation system conditions in power transformers: a view based on practical experience," in *Proceedings of the Electrical Insulation Conference and Electrical Manufacturing & Coil Winding Conference*, pp. 659-667, (1999).

2. A. K. Lokhanin, G. Y. Shneider, V. V. Sokolov, and V. M. Chornogotsky, "Internal insulation failure mechanisms of HV equipment under service conditions," in *CIGRE Report 15-201*, (2002).

3. H. Zainuddin, P.M. Mitchinson and P.L. Lewin, "Investigation on the surface discharge phenomenon at the oil-pressboard interface," in *17th IEEE International Conference on Dielectric Liquids,* (2011).

4. H. Zainuddin, P.L. Lewin and P.M. Mitchinson, "Partial discharge characteristics of surface tracking on oil-impregnated pressboard under AC voltages," in *IEEE 2013 International Conference on Solid Dielectrics,* pp. 1016-1019, (2013).

5. J. Dai, Z. D. Wang, and P. Jarman, "Creepage discharge on insulation barriers in aged power transformers," *IEEE Transactions on Dielectrics and Electrical Insulation,* vol. 17, pp. 1327-1335, (2010).

6. H. Zainuddin, P.L. Lewin and P.M. Mitchinson, "Characteristics of leakage current during surface discharge at the oil-pressboard interface," in *2012 IEEE Conference on Electrical Insulation and Dielectric Phenomena,* pp. 483-486, (2012).

7. P. M. Mitchinson, P. L. Lewin, B. D. Strawbridge, and P. Jarman, "Tracking and surface discharge at the oil-pressboard interface," *IEEE Electrical Insulation Magazine,* vol. 26, pp. 35-41, (March/April 2010).

8. P. H. Rieger, *Electrochemistry*, Prentice-Hall International, Inc., (1987).

9. H. Zainuddin, "Study of surface discharge behaviour at the oil-pressboard interface," PhD thesis, University of Southampton, (2013).

10. J. C. Devins, S. J. Rzad, and R. J. Schwabe, "Breakdown and prebreakdown phenomena in liquids," *Journal of Applied Physics,* vol. 52, pp. 4531-4545, (1981).

11. C. Zener, "A theory of the electrical breakdown of solid dielectrics," *Proceedings of the Royal Society of London. Series A,* vol. 145, pp. 523-529, (1934).

12. J. G. Hwang, M. Zahn, and L. A. A. Pettersson, "Mechanisms behind positive streamers and their distinct propagation modes in tansformer oil," *IEEE Transactions on Dielectrics and Electrical Insulation,* vol. 19, pp. 162-174, (2012).

13. J. Jadidian, M. Zahn, N. Lavesson, O. Widlund, and K. Borg, "Effects of impulse voltage polarity, peak amplitude and rise time on streamers initiated from a needle electrode in transformer oil," *IEEE Transactions on Plasma Science,* vol. 40, pp. 909-918, (2012).

14. W. F. Schmidt, *Liquid State Electronics of Insulating Liquids*, CRC Press, (1997).

15. J. W. G. Hwang, "Elucidating the mechanism behind pre-breakdown phenomena in transformer oil systems," PhD thesis, Massachusetts Institute of Technology, (2010).

16. D. F. Arseneau, "Competitive reactions in the thermal decomposition of cellulose," *Canadian Journal of Chemistry,* vol. 49, pp. 632-638, (1971).

6. Acknowledgements